

The quasi-persistent neutron star soft X-ray transient 1M 1716–315 in quiescence

P.G. Jonker^{1,2,3*}, C.G. Bassa³, S. Wachter⁴

¹SRON, Netherlands Institute for Space Research, Sorbonnelaan 2, 3584 CA, Utrecht, The Netherlands

²Harvard-Smithsonian Center for Astrophysics, 60 Garden Street, Cambridge, MA 02138, Massachusetts, U.S.A.

³Astronomical Institute, Utrecht University, P.O.Box 80000, 3508 TA, Utrecht, The Netherlands

⁴Spitzer Science Center, California Institute of Technology, 1200 E. California Blvd., Pasadena CA 91125, U.S.A.

27 October 2018

ABSTRACT

We report on our analysis of a 20 ksec *Chandra* X-ray observation of the quasi-persistent neutron star soft X-ray transient (SXT) 1M 1716–315 in quiescence. Only one source was detected in the HEAO-I error region. Its luminosity is $1.6 \times 10^{32} - 1.3 \times 10^{33}$ erg s^{−1}. In this the range is dominated by the uncertainty in the source distance. The source spectrum is well described by an absorbed soft spectrum, e.g. a neutron star atmosphere or black body model. No optical or near-infrared counterpart is present at the location of the X-ray source, down to a magnitude limit of $I \gtrsim 23.5$ and $K_s \gtrsim 19.5$. The positional evidence, the soft X-ray spectrum together with the optical and near-infrared non-detections provide strong evidence that this source is the quiescent neutron star SXT. The source is 10–100 times too bright in X-rays in order to be explained by stellar coronal X-ray emission. Together with the interstellar extinction measured in outburst and estimates for the source distance, the reported optical and near-infrared limit give an upper limit on the absolute magnitude of the counterpart of $I > 8.6$ and $K_s > 5.1$. This implies that the system is either an ultra-compact X-ray binary having $P_{\text{orb}} < 1$ hr or the companion star is an M-dwarf. We reconstructed the long term X-ray lightcurve of the source. 1M 1716–315 has been active for more than 12 years before returning to quiescence, the reported *Chandra* observation started 16.9 ± 4.1 years after the outburst ended.

Key words: stars: individual (1M 1716–315) — accretion: accretion discs — stars: binaries — stars: neutron — X-rays: binaries

1 INTRODUCTION

Low-mass X-ray binaries (LMXBs) are highly evolved, interacting binaries in which a neutron star or black hole accretes matter via an accretion disc which is fed by a cool, low-mass star (typically $M \lesssim 1$ M_⊙). Some systems have an orbital period of less than ~ 1 hour (ultra-compact X-ray binaries; UCXBs). These ultra-compact systems are so compact that the donors cannot be main sequence stars, but instead must be hydrogen-poor (semi) degenerate stars (e.g. Verbunt & van den Heuvel 1995). Belczynski & Taam (2004) predict that about half of the total population of LMXBs may be in UCXBs. A large fraction of the LMXBs are found to be transient systems – the so called soft X-ray transients (SXTs; e.g. see Chen et al. 1997).

A special group of soft X-ray transients has several-

year long outbursts before they return to quiescence. These quasi-persistent systems provide an ideal testing ground since the accretion history is well-constraint. Furthermore, the idea is that the long outburst has heated the neutron star crust to temperatures higher than that of the neutron star core. Therefore, the (evolution of the) quiescent X-ray luminosity provides information on the cooling properties of the neutron star, which in turn depend on the neutron star equation of state (Brown et al. 1998; Colpi et al. 2001; Wijnands et al. 2001; Rutledge et al. 2002; Cackett et al. 2006b).

1M 1716–315 was first detected in OSO-7 observations obtained between Sept. 29, 1971 and May 18, 1974 (Markert et al. 1975). The last reported detection was by Warwick et al. (1988) using EXOSAT observations obtained in June 14–18, 1984. The source was not detected by the ROSAT all sky survey (Voges et al. 1999). Large X-ray flares lasting ≈ 10 minutes have been reported

* email : p.jonker@sron.nl

(Markert et al. 1976). These and other (shorter) flares reported by Jernigan et al. (1978) would now most likely be classified as type I X-ray bursts. The confirmation of the occurrence of type I X-ray bursts and hence of the neutron star nature of the compact object in 1M 1716–315 was given by the detection of three bursts by the Hakucho satellite (Makishima et al. 1981). Later Hakucho detected a long radius expansion burst (Tawara et al. 1984b). The properties of this burst were used by Tawara et al. (1984a) to derive a distance of ~ 6 kpc (Jonker & Nelemans 2004 derived $d=5.1\text{--}6.9$ kpc using the properties of the same burst; the range depends on whether the burst was hydrogen or helium rich).

The source position was determined to $90''$ by SAS–3 (90 per cent confidence; Jernigan et al. 1978). The position was later refined by HEAO–I to an area with an equivalent circular radius of $23''$ (90 per cent confidence; Reid et al. 1980). The extinction towards the source is low for an LMXB; Christian & Swank (1997) report an equivalent hydrogen column density of $N_H = (2.1 \pm 0.6) \times 10^{21} \text{ cm}^{-2}$. Wachter et al. (2005) observed the source for 1 ksec. with the High Resolution Camera onboard the *Chandra* satellite but did not detect the source; they report an upper limit on the flux of $2.8 \times 10^{-14} \text{ erg cm}^{-2} \text{ s}^{-1}$. In this Manuscript, we report on a deeper *Chandra* observation of the neutron star soft X-ray transient 1M 1716–315 in quiescence. We further report on optical Magellan and near-infrared Blanco observations obtained while the source was in quiescence.

2 OBSERVATIONS, ANALYSIS AND RESULTS

2.1 X-ray observations

We observed 1M 1716–315 with the back-illuminated S3 CCD-chip of the Advanced CCD Imaging Spectrometer (ACIS) detector on board the *Chandra* satellite. The observations started on MJD 53567.604 (UTC; July 16, 2005). The net, on-source exposure time was ~ 20 ks. The data telemetry mode was set to VERY FAINT to allow for a better background subtraction. After the data were processed by the *Chandra* X-ray Center (ASCS version 7.6.0), we analysed them using the CIAO 3.3 software developed by the *Chandra* X-ray Center. We reprocessed the data to clean the background taking full advantage of the VERY FAINT data mode. We searched the data for background flares but none were found, hence we used all data in our analysis. Using the CIAO tool WAVDETECT we detect and determine positions of 20 sources in the field of view of the ACIS S3 CCD (see Fig. 1 and Table 1).

2.2 Optical observations

In order to search for the optical counterpart in quiescence, we have obtained *I*-band images with the Inamori-Magellan Areal Camera and Spectrograph (IMACS) instrument mounted on the 6.5 m Magellan–Baade telescope on July 7, 2005, 00:00:35 UTC (MJD 53558.0004 UTC). Exposure times of 10 seconds and 2x300 seconds were used. IMACS is a mosaic of eight $4\text{k} \times 2\text{k}$ CCDs that were operated in a 2×2 binning mode. The seeing was $0''.7$. We calibrated all 8 CCD chips of the 10s *I*-band image against stars from

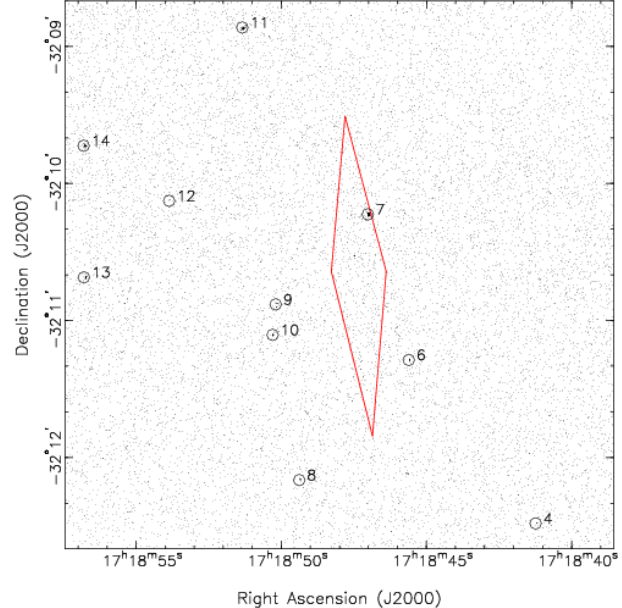


Figure 1. Part ($4' \times 4'$) of *Chandra*'s ACIS–S3 CCD is shown. The diamond shaped region is the HEAO–I error region of 1M 1716–315. Only one of the detected sources is consistent with that position. The circles indicate the positions of detected X-ray sources (see Table 1 for the numbering).

the second version of the USNO CCD Astrograph Catalog (UCAC2; Zacharias et al. 2004). Between 13 and 28 stars were used to compute the transformation for each chip, giving typical root-mean-square residuals of $0''.058$ and $0''.051$ on α and δ , respectively. From the 20 X-ray sources found on the ACIS–S3 chip, 8 coincided with relatively bright stars on the 10s *I*-band image (see Table 1) having *I*-band magnitudes between 11 and 16. The celestial positions of these stars were measured from the calibrated images and compared with the X-ray positions to determine a boresight correction of $\Delta\alpha = -0''.001 \pm 0''.037$ and $\Delta\delta = +0''.016 \pm 0''.035$. Using this boresight correction we obtained positions and uncertainties for the 20 sources detected by *Chandra* on the S3 CCD chip (see Table 1).

Subsequently, the astrometric solution of the 10-second frame was transferred to the 300-second images using ~ 1700 stars. In this the rms uncertainty was $0''.037$ in each coordinate. For the X-ray source in the HEAO–I error region the uncertainty in its location due to the wavelet fitting in WAVDETECT is $0''.045$ in α and $0''.038$ in δ . Adding all the errors in quadrature gives at the 99% confidence level an radius for the error circle of $0''.36$. The images have been corrected for bias and flatfielded with IRAF¹.

2.3 Near-infrared observations

We have also obtained near-IR *K_s* band data with the Blanco 4 m telescope and Infrared Side Port Imager (ISPI) at Cerro Tololo Inter-American Observatory (CTIO) on 2004 July 25 UTC. The observation consists of three 20 sec

¹ IRAF is distributed by the National Optical Astronomy Observatories

Table 1. Names, coordinates and detection significance of the 20 sources detected by *Chandra* on the S3 CCD chip sorted on Right Ascension.

Number & Name	α (h:m:s \pm "", J2000.0)	δ ($^{\circ}$: $'$: $''$ \pm "", J2000.0)	σ
1 CXOU J171830.7-320927 ^c	17:18:30.69 \pm 0.18	-32:09:27.31 \pm 0.13	11.9
2 CXOU J171833.1-320630 ^{b,c}	17:18:33.10 \pm 0.10	-32:06:30.85 \pm 0.08	44.2
3 CXOU J171836.0-320940 ^c	17:18:36.01 \pm 0.13	-32:09:40.40 \pm 0.11	17.1
4 CXOU J171841.2-321228	17:18:41.24 \pm 0.19	-32:12:28.90 \pm 0.19	5.1
5 CXOU J171842.4-320643 ^c	17:18:42.40 \pm 0.32	-32:06:43.74 \pm 0.18	7.1
6 CXOU J171845.6-321117	17:18:45.61 \pm 0.12	-32:11:17.32 \pm 0.17	7.1
7 CXOU J171847.0-321013 ^a	17:18:47.02 \pm 0.08	-32:10:13.54 \pm 0.07	41.9
8 CXOU J171849.4-321209	17:18:49.38 \pm 0.14	-32:12:09.93 \pm 0.13	7.8
9 CXOU J171850.2-321053	17:18:50.19 \pm 0.16	-32:10:53.03 \pm 0.19	4.8
10 CXOU J171850.3-321106	17:18:50.30 \pm 0.20	-32:11:06.35 \pm 0.22	4.8
11 CXOU J171851.3-320851 ^b	17:18:51.34 \pm 0.15	-32:08:51.77 \pm 0.11	12.3
12 CXOU J171853.9-321007	17:18:53.86 \pm 0.23	-32:10:07.64 \pm 0.24	4.6
13 CXOU J171856.8-321041 ^b	17:18:56.80 \pm 0.14	-32:10:41.14 \pm 0.14	9.5
14 CXOU J171856.8-320943 ^b	17:18:56.81 \pm 0.13	-32:09:43.55 \pm 0.14	11.2
15 CXOU J171858.0-320932 ^c	17:18:58.00 \pm 0.27	-32:09:32.44 \pm 0.28	4.6
16 CXOU J171859.2-321147 ^{b,c}	17:18:59.22 \pm 0.10	-32:11:47.86 \pm 0.10	16.1
17 CXOU J171900.2-320958 ^c	17:19:00.25 \pm 0.23	-32:09:58.98 \pm 0.22	5.2
18 CXOU J171903.3-321123 ^{b,c}	17:19:03.30 \pm 0.11	-32:11:23.40 \pm 0.11	26.8
19 CXOU J171903.4-320925 ^{b,c}	17:19:03.35 \pm 0.20	-32:09:25.24 \pm 0.21	7.6
20 CXOU J171905.0-321023 ^{b,c}	17:19:04.98 \pm 0.11	-32:10:23.14 \pm 0.11	21.5

^a 1M 1716–315 in quiescence.

^b Bright optical star at the X-ray position used for boresight correction.

^c This source is outside the field shown in Figure 1.

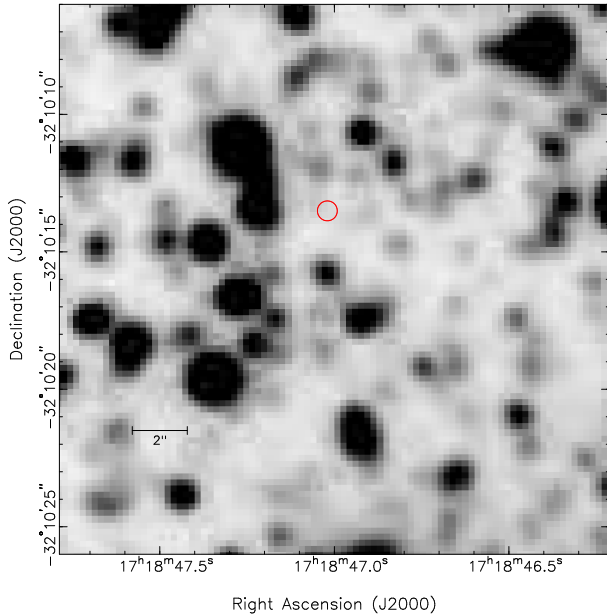


Figure 2. An I -band finder chart of the field of 1M 1716–315 obtained with Magellan/IMACS (North is up and East is left). The small circle indicates the position of the *Chandra* detected X-ray source number 7 (radius error circle $0''.36$, 99 per cent confidence).

coadds at nine dither positions. The data were flatfielded, sky background subtracted and combined into a single final image in the standard manner using IRAF. ISPI has a pixel scale of $0''.3$ pixel $^{-1}$ and the seeing conditions during the observations varied between $0''.9$ – $1''.0$. We have derived a photometric calibration transformation for the final combined image based on a comparison to 2MASS measurements, neglecting any colour terms since we only have data in one

filter. The formal rms error in the transformation fit was 0.04 mag.

2.4 The quiescent X-ray counterpart to 1M 1716–315?

Only one source is detected in the HEAO-I error region of 1M 1716–315 (source number 7 in Table 1). Hence, source 7 is a strong counterpart candidate. In the error circle of source 7 on the optical I -band image there is no object present. We estimate a 5σ detection limit of $I > 23.5$ (see Jonker et al. 2006). Furthermore, no K_s counterpart is detected in the *Chandra* error circle and we estimate a detection limit of $K_s > 19.5$. There are three other sources detected in X-rays that have a position close to the error region (sources 6, 9 and 10 using the numbering from Table 1 in Figure 1). For none of these sources we detected the I - or K_s -band counterpart. In the case of the X-ray source number 9 a bright source was present both in the I - and the K_s -band image at a location close to, but not consistent with, its *Chandra* error circle. The wings of the psf of the bright star, however, cover the *Chandra* error circle of source number 9 raising the level of the background considerably. This precludes us from putting firm limits on the presence of a star at the position of the X-ray source number 9. Hence, on the basis of the optical to X-ray luminosity ratio one can not rule out any of these sources as the potential counterpart of 1M 1716–315. Furthermore, the X-ray source in the error circle could in principle be unrelated to 1M 1716–315: the quiescent X-ray counterpart of 1M 1716–315 could be fainter than our detection limit. In a $1''$ circle, placed randomly in the HEAO-I error region we find 0–3 counts. Using the conservative limit of 3 counts and (Gehrels 1986) this converts to a 95 per cent count rate upper limit of 3.9×10^{-4} counts s $^{-1}$. For a power law with

index 2 and an $N_H = 2.1 \times 10^{21} \text{ cm}^{-2}$ this yields a $3 \times 10^{-15} \text{ erg cm}^{-2} \text{ s}^{-1}$ limit on the 0.5–10 keV flux. For a distance of 6.9 kpc this gives a limit on the 0.5–10 keV luminosity of $2 \times 10^{31} \text{ erg s}^{-1}$.

2.5 The X-ray spectrum and lightcurve

We extracted the X-ray photons from a circular region with a diametre of 3'' of source 7, 6, 9 and 10. For source 7, background photons were extracted from an annulus centred on the source with an inner and outer radius of 10'' and 40'', respectively. For source 7 we detect 185 source photons in the 19,924-seconds long effective exposure. Hence, the source count rate is $(9.3 \pm 0.7) \times 10^{-3} \text{ counts s}^{-1}$. The lightcurve of the source is consistent with being constant. At these low background-subtracted count rates, photon pile-up is unimportant. We searched for spectral variability during the observation by comparing the mean energy and the variance therein of the photons in the first half of the observation with that of the second half. The two values are consistent with being the same. Even though the shape of the spectrum can have changed keeping the mean energy and its variance constant, it is more likely that within the accuracy of our data the spectrum did not change during the observation. In order to validate the use of the χ^2 fitting technique in the spectral analysis, the source spectrum was rebinned such that each of the spectral bins contained at least 10 counts.

The 0.3–10 keV X-ray spectrum was fitted with XSPEC 11.3.1 (Arnaud 1996). The fit function consists of either an absorbed neutron star atmosphere (NSA; Pavlov et al. 1991; Zavlin et al. 1996), black body or power law model. Each of these absorbed models provides an acceptable fit to the X-ray spectrum in terms of reduced χ^2 . However, the best-fit power law index was very high with $6.4^{+1.1}_{-0.8}$ and the interstellar extinction was $1.5 \pm 0.3 \times 10^{22} \text{ cm}^{-2}$ in this case, higher than the best-fit value found in outburst (errors here and below are at the 68 per cent confidence level). For these reasons we do not consider the single absorbed power law model any further. We provide the best-fit parameters for the black body and the NSA model in Table 2 (see also Figure 3). In order to determine the upper limit on the contribution of a powerlaw to the 0.5–10 keV X-ray flux, we determine the best-fit using a model without a power-law. Next, we fix all the parameters related to this model and add a power-law to the fit function. The power-law index is fixed to the value 2. Hence, the only free parameter is the power-law normalisation. After fitting we determine the 90 per cent confidence error. The outcome of the error in the positive scan direction is added to the value of the power-law normalisation. The normalisation of the other model components is set to zero as well as the parameter for the interstellar extinction. Subsequently, the flux in only the power-law component is derived. Finally, this flux is expressed as a fraction of the flux in the other model components. We give this 95 per cent confidence upper limit in between brackets in Table 2.

For sources 6, 9 and 10 we only detected 24, 14 and 13 photons in the energy range 0.3–10 keV in the 3'' source area, respectively. Out of these there are approximately 7 ± 3 background photons. We have tried to model the X-ray spectra in XSPEC 11.3.1 making use of the C-statistics, however, the model parameters are unconstrained. In order to investigate the spectral properties of these sources, keeping in mind that

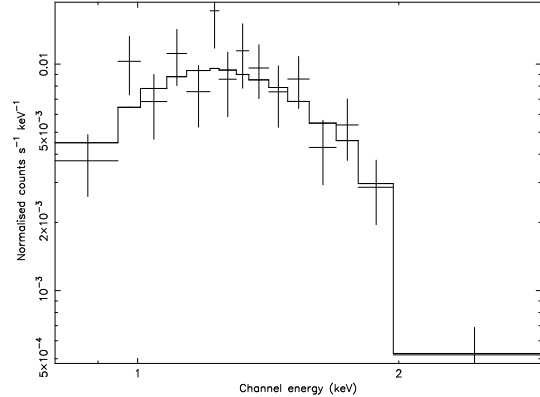


Figure 3. The 0.5–10 keV X-ray spectrum of 1M 1716–315 (source 7) in quiescence obtained with *Chandra*'s ACIS-S on MJD 53567.604 (UTC; July 16, 2005). The solid line represents the best-fit absorbed NSA model where N_H is a free-floating fit parameter.

the background photons generally have a hard spectrum, we determine the number of photons in the 0.3–1.5 keV and 1.5–10 keV energy band and the mean energy in the 0.3–1.5 keV and 1.5–10 keV bands. For sources 6, 9, and 10 we find 7/17, 2/12 and 2/11 photons in the 0.3–1.5 keV/1.5–10 keV band, respectively. The mean 0.3–1.5 keV/1.5–10 keV energy and the variance therein for source 6, 9 and 10 is $1.2 \pm 0.3 \text{ keV}/3.3 \pm 2.2 \text{ keV}$, $1.2 \pm 0.1 \text{ keV}/4.6 \pm 2.7 \text{ keV}$ and $1.0 \pm 0.2 \text{ keV}/4.4 \pm 2.4 \text{ keV}$, respectively. One can not exclude sources 6, 9 and 10 on the basis of their hard spectra alone as possible quiescent counterparts of the neutron star SXT 1M 1716–315 since some neutron stars have been found to have a hard spectrum at low luminosities in quiescence (see e.g. Jonker et al. 2004). However, only source 7 has a spectrum that is consistent with a soft spectrum as often found for a quiescent neutron star. Whereas coronal activity from a star might also yield a soft spectrum (for a review see Güdel 2004), we find no evidence in the optical nor near-infrared for the presence of such a star. From figure 2 in Güdel (2004), the observational *I*-band limit and the observed X-ray flux it can be derived that in order to explain the X-ray emission as coronal X-ray emission of a star, that star would need to be several orders of magnitude brighter than has been found before in order to explain the observed X-ray flux and the optical non-detection. This makes the identification of the X-ray source as stellar coronal X-ray emission unlikely. Instead, we conclude that based on the positional coincidence, the spectral properties together with the optical and near-infrared upper limits, it is very likely that source 7 is the quiescent neutron star counterpart to 1M 1716–315.

With the new accurate *Chandra* X-ray position from our ACIS-S observation in hand, we re-analysed the HRC-I observation of Wachter et al. (2005). Only one photon is detected in the 0''.67 90 per cent confidence error circle centred on the best-fit source position (taking into account the nominal 0''.6 90 per cent error for *Chandra* observations since we could not correct the bore sight for the *Chandra*-HRC observation). Using Gehrels (1986) this gives a 95 per cent confidence upper limit on the source count rate of $4 \times 10^{-3} \text{ counts s}^{-1}$. Assuming the same spectral energy distribution as found from our *Chandra* ACIS-S observation and fixing

Table 2. Best fit parameters of the quiescent spectrum of 1M 1716–315. NSA stands for neutron star atmosphere and BB refers to blackbody. All quoted errors are at the 68 per cent confidence level. The value in between brackets in the unabsorbed flux column denotes the 95 per cent upper limit to the fractional contribution of a power law (the power law index was fixed at 2; see text).

Model	$N_H \times 10^{21}$ cm $^{-2}$	BB radius $(\frac{d}{10 \text{ kpc}})^2$ km	NSA norm. d (kpc)	Temp. BB (keV)/NSA $\log K/\text{keV}^\infty$	Unabs. 0.5–10 keV flux (erg cm $^{-2}$ s $^{-1}$)	Abs. 0.5–10 keV flux (erg cm $^{-2}$ s $^{-1}$)	χ^2_{red} d.o.f.
BB	2.1 ^a	0.4±0.1	–	0.33±0.02	$(5.0^{+0.3}_{-0.8}) \times 10^{-14}$ (19%)	$(3.3^{+0.2}_{-0.4}) \times 10^{-14}$	1.16/13
NSA	2.1 ^a	–	53±11	$6.42 \pm 0.04 / 0.17 \pm 0.02$	$(5.4^{+2.3}_{-2.6}) \times 10^{-14}$ (18%)	$(3.7^{+1.2}_{-1.6}) \times 10^{-14}$	1.39/13
BB	7±2	5 ⁺⁹ ₋₅	–	0.24±0.03	$(1.3^{+0.1}_{-0.6}) \times 10^{-13}$ (16%)	$(3.1^{+0.1}_{-1.4}) \times 10^{-14}$	0.64/12
NSA	9±2	–	3.9 ^{+b} _{-2.3}	$6.07 \pm 0.08 / 0.078 \pm 0.014$	$(2.4^b) \times 10^{-13}$ (8%)	$(3.2^b) \times 10^{-14}$	0.63/12

^a Parameter fixed.

^b Error range is unconstrained.

N_H to 2.1×10^{21} cm $^{-2}$, the 95 per cent confidence upper limit on the unabsorbed 0.5–10 keV source flux is 5.6×10^{-14} erg cm $^{-2}$ s $^{-1}$, slightly higher than that derived by Wachter et al. (2005; in this we used w3pimms²). The upper limit on the flux derived from the *Chandra* HRC–I observation is consistent with the flux measured in our ACIS–S observation.

3 DISCUSSION

We have observed the field of the neutron star SXT 1M 1716–315 in X–rays with the *Chandra* satellite for ~ 20 ksec. We detect only one source in the HEAO–I error region. The spectrum of the source is soft with a 95 per cent upper limit to a power law contribution of < 19 per cent making it unlikely that this source is a background AGN or an accreting white dwarf. The X–ray luminosity together with our stringent optical I –band and near–infrared K_s –band limits on the absolute magnitude rule out that the soft X–ray spectrum is due to coronal activity of a late type star. Three other sources were found near the 90 per cent confidence HEAO–I error region. Even though the detected number of counts for these sources is too low to fit a spectrum nearly all photons of all three sources are detected above 1.5 keV. Together with the fact that their positions do not agree with the HEAO–I error region, this makes them less likely candidates for the quiescent neutron star SXT.

We conclude that we have detected 1M 1716–315 in quiescence at a 0.5–10 keV source luminosity of $1.6 \times 10^{32} – 1.3 \times 10^{33}$ erg s $^{-1}$. Fixing the value for the interstellar N_H to the value given in Christian & Swank (1997) [$(2.1 \pm 0.6) \times 10^{21}$ cm $^{-2}$] the resultant blackbody and neutron star atmosphere temperature is rather high for a neutron star SXT in quiescence, especially when taking into account that the source has been in quiescence for more than ≈ 16 years (see below). We note that the N_H value given in table 12 of Christian & Swank (1997) depends on the spectral model that was used, both an absorbed blackbody plus thermal bremsstrahlung as well as Comptonisation models give a N_H value of $4–5 \times 10^{21}$ cm $^{-2}$ (see tables 7 and 10 in Christian & Swank 1997). Indeed, when left as a free parameter in our X–ray spectral fits the N_H is somewhat higher, although still consistent within 3 σ with the value of $(2.1 \pm 0.6) \times 10^{21}$ cm $^{-2}$.

The I –band observations do not reveal an optical counterpart in the 99 per cent confidence 0''.36 error circle down to a magnitude limit of $I > 23.5$. Using this limit and converting the N_H observed in outburst giving $A_I \sim 0.7$ (Schlegel et al. 1998), taking $d=5.1–6.9$ kpc (Jonker & Nelemans 2004) we derive that the absolute I –band magnitude $M_I \geq 8.6 – 9.3$. Equivalent calculations for the K_s band measurements result in $K_s \geq 5.1 – 5.8$. Hence, like 1H 1905+000 (Jonker et al. 2006) 1M 1716–315 is a candidate UCXB, although the secondary could also be an M dwarf. However, additional (circumstantial) evidence for an ultra–compact nature comes from the detected long (≈ 10 minutes) type I burst duration (Markert et al. 1976). Such long bursts can occur in sources accreting He at a low rate in ultra–compact X–ray binaries (see discussion in in't Zand et al. 2007) or sources accreting H–rich material at even lower rates (Peng et al. 2007). Since the luminosity in outburst in the case of 1M 1716–315 was found to be above 10^{36} erg s $^{-1}$ the latter mode is less likely. The quiescent X–ray luminosity of 1M 1716–315 is higher than that of other (likely) UCXBs in quiescence (XTE J1751–305, XTE J0929–314, XTE J1807–294, and 1H 1905+000; Wijnands et al. 2005; Campana et al. 2005; Jonker et al. 2006). A plausible explanation for the higher quiescent luminosity is that the time–averaged mass accretion rate is higher in 1M 1716–315 than in the other UCXBs observed so far, possibly due to a shorter orbital period (Deloye & Bildsten 2003).

We have plotted the long–term lightcurve of 1M 1716–315 in Figure 4.³ The most striking feature is the longevity of the outburst. The source has been active for nearly 13 years before it returned to quiescence (Fig. 4). There is a time span of 8.2 years between the last detection by EXOSAT and the first non–detection by ROSAT. The source is likely to have returned to quiescence during this interval. There is 16.9 years between the mid–point of this interval and the time of the *Chandra* observation that detected the source. Hence, the source has been in quiescence for 16.9 ± 4.1 years. There is a growing number of quasi–persistent sources (the other

³ Data for Figure 4 was taken or derived from Forman et al. (1978) (UHURU); Markert et al. (1975), Markert et al. (1976) and Markert et al. (1977) (OSO–7), Jernigan et al. (1978) (SAS–3), Reid et al. (1980) (HEAO–I), Christian & Swank (1997) (Einstein), Warwick et al. (1988) and Gottwald et al. (1995) (EXOSAT), Voges et al. (1999) (ROSAT), and this work

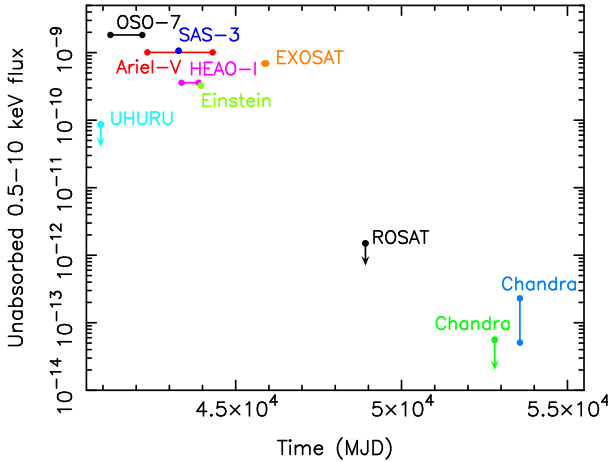


Figure 4. The unabsorbed 0.5–10 keV X-ray flux history of the source 1M 1716–315. The plotted ranges for each satellite indicate the time span over which the source was detected on multiple occasions by that satellite. In order to convert fluxes given in the literature in other X-ray bands to the 0.5–10 keV band we assume the spectrum to be well-represented by an absorbed power law with index 2 (except for the ROSAT and *Chandra* upper limit which were derived assuming a 0.3 keV black body). The absorption was taken to be $2.1 \times 10^{21} \text{ cm}^{-2}$ as found from spectra obtained in outburst by Einstein (Christian & Swank 1997). Arrows on the data points indicate upper limits to the X-ray flux.

sources being 2S 1711–339⁴, 4U 2129+47, KS 1731–260, MXB 1659–290, X 1732–304, and 1H 1905+000, Wijnands 2004; Torres et al. 2004; Cackett et al. 2006c; Cackett et al. 2006a; Jonker et al. 2006). Of these, only 1H 1905+000 has so far not been detected in quiescence. At present there are three other quasi-persistent sources that are still in outburst, EXO 0748–676, GS 1826–238, and XTE J1759–220. In addition, HETE J1900.1–2455 has been in outburst for more than a year now. All these quasi-persistent sources have confirmed neutron star accretors, except XTE J1759–220 for which type I bursts or pulsations have not been reported so far.

ACKNOWLEDGMENTS

PGJ and SW acknowledges support from NASA grant GO4-5033X. PGJ and CGB acknowledge support from the Netherlands Organisation for Scientific Research. We also acknowledge Frank Verbunt for useful discussions and the referee for useful comments that helped improve the manuscript.

REFERENCES

Arnaud, K. A., 1996, in ASP Conf. Ser. 101: Astronomical Data Analysis Software and Systems V, vol. 5, p. 17

Belczynski, K., Taam, R. E., 2004, ApJ, 603, 690

⁴ This source has had a $\gtrsim 3$ year-long outburst between MJD 50,739 and 51,751. On MJD 52,345 it was not detected with *Chandra* (see also Wilson et al. 2003).

Brown, E. F., Bildsten, L., Rutledge, R. E., 1998, ApJ, 504, L95

Cackett, E. M., Wijnands, R., Linares, M., Miller, J. M., Homan, J., Lewin, W., 2006a, ArXiv Astrophysics e-prints

Cackett, E. M., Wijnands, R., Linares, M., Miller, J. M., Homan, J., Lewin, W. H. G., 2006b, MNRAS, 372, 479

Cackett, E. M., et al., 2006c, MNRAS, 479

Campana, S., Ferrari, N., Stella, L., Israel, G. L., 2005, A&A, 434, L9

Chen, W., Shrader, C. R., Livio, M., 1997, ApJ, 491, 312

Christian, D. J., Swank, J. H., 1997, ApJS, 109, 177

Colpi, M., Geppert, U., Page, D., Possenti, A., 2001, ApJ, 548, L175

Deloye, C. J., Bildsten, L., 2003, ApJ, 598, 1217

Forman, W., Jones, C., Cominsky, L., Julien, P., Murray, S., Peters, G., Tananbaum, H., Giacconi, R., 1978, ApJS, 38, 357

Gehrels, N., 1986, ApJ, 303, 336

Gottwald, M., Parmar, A. N., Reynolds, A. P., White, N. E., Peacock, A., Taylor, B. G., 1995, A&AS, 109, 9

Güdel, M., 2004, ARA&A, 42, 71

in't Zand, J. J. M., Jonker, P. G., Markwardt, C. B., 2007, A&A

Jernigan, J. G., Bradt, H. V., Doxsey, R. E., Dower, R. G., McClintock, J. E., Apparao, K. M. V., 1978, Nat, 272, 701

Jonker, P. G., Nelemans, G., 2004, MNRAS, 354, 355

Jonker, P. G., Galloway, D. K., McClintock, J. E., Buxton, M., Garcia, M., Murray, S., 2004, MNRAS, 354, 666

Jonker, P. G., Bassa, C. G., Nelemans, G., Juett, A. M., Brown, E. F., Chakrabarty, D., 2006, MNRAS, 395

Makishima, K., et al., 1981, ApJ, 244, L79

Markert, T. H., Bradt, H. V., Clark, G. W., Lewin, W. H. G., Li, F. K., Schnopper, H. W., Sprott, G. F., Wargo, G. F., 1975, IAU Circ, 2765, 1

Markert, T. H., Backman, D. E., McClintock, J. E., 1976, ApJ, 208, L115

Markert, T. H., Canizares, C. R., Clark, G. W., Hearn, D. R., Li, F. K., Sprott, G. F., Winkler, P. F., 1977, ApJ, 218, 801

Pavlov, G. G., Shibanov, I. A., Zavlin, V. E., 1991, MNRAS, 253, 193

Peng, F., Brown, E. F., Truran, J. W., 2007, ApJ, 654, 1022

Reid, C. A., Johnston, M. D., Bradt, H. V., Doxsey, R. E., Griffiths, R. E., Schwartz, D. A., 1980, AJ, 85, 1062

Rutledge, R. E., Bildsten, L., Brown, E. F., Pavlov, G. G., Zavlin, V. E., Ushomirsky, G., 2002, ApJ, 580, 413

Schlegel, D. J., Finkbeiner, D. P., Davis, M., 1998, ApJ, 500, 525

Tawara, Y., Hirano, T., Kii, T., Matsuoka, M., Murakami, T., 1984a, PASJ, 36, 861

Tawara, Y., et al., 1984b, ApJ, 276, L41

Torres, M. A. P., McClintock, J. E., Garcia, M. R., Murray, S. S., 2004, The Astronomer's Telegram, 233, 1

Verbunt, F., van den Heuvel, E., 1995, Formation and evolution of neutron stars and black holes in binaries, eds Lewin, van Paradijs, van den Heuvel, ISBN 052141684, Cambridge University Press, 1995.

Voges, W., et al., 1999, A&A, 349, 389

Wachter, S., Wellhouse, J. W., Bandyopadhyay, R. M., 2005, in Burderi, L., Antonelli, L. A., D'Antona, F., di Salvo, T., Israel, G. L., Piersanti, L., Tornambè, A.,

Straniero, O., eds., AIP Conf. Proc. 797: Interacting Binaries: Accretion, Evolution, and Outcomes, p. 639

Warwick, R. S., Norton, A. J., Turner, M. J. L., Watson, M. G., Willingale, R., 1988, MNRAS, 232, 551

Wijnands, R., 2004, in Crust cooling curves of accretion-heated neutron stars, p. 1624

Wijnands, R., Miller, J. M., Markwardt, C., Lewin, W. H. G., van der Klis, M., 2001, ApJ, 560, L159

Wijnands, R., Homan, J., Heinke, C. O., Miller, J. M., Lewin, W. H. G., 2005, ApJ, 619, 492

Wilson, C. A., Patel, S. K., Kouveliotou, C., Jonker, P. G., van der Klis, M., Lewin, W. H. G., Belloni, T., Méndez, M., 2003, ApJ, 596, 1220

Zacharias, N., Urban, S. E., Zacharias, M. I., Wycoff, G. L., Hall, D. M., Monet, D. G., Rafferty, T. J., 2004, AJ, 127, 3043

Zavlin, V. E., Pavlov, G. G., Shibanov, Y. A., 1996, A&A, 315, 141